HHS Public Access

Author manuscript

Neurocrit Care. Author manuscript; available in PMC 2017 June 20.

Published in final edited form as:

Neurocrit Care. 2016 June ; 24(3): 324–331. doi:10.1007/s12028-016-0245-y.

Metabolic Correlates of the Ictal-Interictal Continuum: FDG-PET During Continuous EEG

Aaron F. Struck[1], **M. Brandon Westover**[1], **Lance T. Hall**[2], **Gina M. Deck**[1], **Andrew J. Cole**[1], and **Eric S. Rosenthal**[1]

[1]Department of Neurology, Massachusetts General Hospital (MGH), 55 Fruit Street, Wang 735, Boston, MA 02114, USA

[2]Department of Radiology, University of Wisconsin, Madison, WI, USA

Abstract

Background—Ictal-interictal continuum (IIC) continuous EEG (cEEG) patterns including periodic discharges and rhythmic delta activity are associated with poor outcome and in the appropriate clinical context, IIC patterns may represent "electroclinical" status epilepticus (SE). To clarify the significance of IIC patterns and their relationship to "electrographic" SE, we investigated FDG-PET imaging as a complementary metabolic biomarker of SE among patients with IIC patterns.

Methods—A single-center prospective clinical database was ascertained for patients undergoing FDG-PET during cEEG. Following MRI-PET co-registration, the maximum standardized uptake value in cortical and subcortical regions was compared to contralateral homologous and cerebellar regions. Consensus cEEG review and clinical rating of etiology and treatment response were performed retrospectively with blinding. Electrographic SE was classified as discrete seizures without interictal recovery or >3-Hz rhythmic IIC patterns. Electroclinical SE was classified as IIC patterns with electrographic and clinical response to anticonvulsants; clonic activity; or persistent post-ictal encephalopathy.

Results—Eighteen hospitalized subjects underwent FDG-PET during contemporaneous IIC patterns attributed to structural lesions (44 %), neuroinflammatory/neuroinfectious disease (39 %), or epilepsy (11 %). FDG-PET hypermetabolism was common (61 %) and predicted electrographic or electroclinical SE (sensitivity 79 % [95 % CI 53–93 %] and specificity 100 % [95 % CI 51–100 %]; $p = 0.01$). Excluding electrographic SE, hypermetabolism also predicted electroclinical SE (sensitivity 80 % [95 % CI 44–94 %] and specificity 100 % [95 % CI 51–100 %]; $p = 0.01$).

Correspondence to: Aaron F. Struck.

Compliance with Ethical Standards

Disclosures Aaron F Struck, MD: Dr. Struck reports no disclosures. M. Brandon Westover, MD PhD: Dr. Westover receives funding from NIH-NINDS (K23 NS090900), the Rappaport Foundation, and the Andrew David Heitman Neuroendovascular Research Fund. Lance Hall, MD: receives research funding from, R01 CA158800-01 (NIH/NCI), R21 CA198392-01 (NIH/NCI), Merck/GE Healthcare. Gina M Deck, MD: Dr. Deck reports no disclosures. Andrew J Cole, MD: Dr. Cole reports no disclosures. Eric S. Rosenthal, MD: Dr. Rosenthal receives research support from an institutional contract with SAGE Therapeutics, and Grant funding from the Andrew David Heitman Neuroendovascular Research Foundation, NIBIB (5U54EB007954-04), NINDS (5U10NS080369-02), and the U.S. Army Medical Research and Materiel Command (W81XWH-08-2-0154).

Conclusions—In hospitalized patients with IIC EEG patterns, FDG-PET hypermetabolism is common and is a candidate metabolic biomarker of electrographic SE or electroclinical SE.

Keywords

FDG-PET; EEG; Status epilepticus; Ictal-interictal continuum

Introduction

Continuous electroencephalography (cEEG) commonly identifies periodic and rhythmic patterns on the ictal-interictal continuum (IIC) in patients with neurologic injury [1]. IIC patterns are associated with poor neurologic outcome [2–4], even in the absence of electrographic status epilepticus (SE). The significance of these patterns in relation to cerebral dysfunction and neurologic injury remains unclear [5].

Electrographic SE represents the transition from an indeterminate EEG pattern, that is, an IIC pattern, to a definitively ictal pattern and electrographic SE is associated with significant morbidity and mortality [6, 7]. However, IIC patterns without definite electrographic status epilepticus on scalp EEG are often observed in relation to clonic movements, encephalopathy following status epilepticus [8] or synchronized with depth seizures in the setting of coma [9]. As a result, IIC patterns are often managed as electroclinical SE in the appropriate clinical context, and may respond to anti-epileptic drugs (AEDs).

Measurements of metabolism in patients with IIC patterns may offer information complementary to and distinct from EEG activity. ^{18}F-Fluorodeoxyglucose positron emission tomography (FDG-PET) represents an opportunity to further characterize the metabolic impact of IIC patterns potentially signifying neuronal injury or metabolic stress that might guide treatment. FDG-PET measures glucose uptake and commonly demonstrates hypermetabolism during seizures and status epilepticus [10–15], while AQ infarcted cerebral tissue manifests reduced glucose uptake. Most cerebral metabolic activity (80–85 %) is related to propagation of action potentials and restoring post-synaptic ion fluxes primarily related to glutamate, making metabolism a fairly direct measure of neuronal activity [16]. There have only been single case reports demonstrating FDG-PET metabolic changes corresponding to IIC patterns [10, 17–19]. We therefore investigated FDG-PET cerebral metabolism as a candidate biomarker for electrographic SE or electroclinical SE among patients with IIC patterns.

Methods

Subjects

After local institutional review board approval, a single-center prospective clinical EEG database was queried for inpatients between 2005 and 2014 undergoing cEEG and cerebral FDG-PET. Inclusion criteria included FDG-PET imaging available for analysis, raw structural imaging available for anatomic co-registration, cEEG performed immediately prior to and immediately after FDG-PET imaging, and presence of IIC patterns: periodic discharges (PD), rhythmic delta activity (RDA), spike-wave activity (SW), or electrographic

SE on cEEG at the time of PET injection. We excluded patients undergoing FDG-PET for elective characterization of chronic epilepsy.

FDG-PET Acquisition

PET imaging was performed under standard protocol, 45 min after injection of 5.0 mCi of FDG, and acquired on an ECAT HR+ scanner (Siemens/CTI, Knoxville, TN). A 15.5-cm field of view was acquired with sixty-three planes simultaneously in 3D mode. For attenuation correction a transmission scan with a ^{68}Ge source was used. Reconstruction was performed using a maximum likelihood algorithm. Images had approximately 4.6-mm resolution at full width at half maximum.

PET Interpretation

An investigator blinded to the cEEG results used a semi-quantitative method to define the degree and extent of FDG-PET uptake. This analysis was performed blinded to the initial "clinical" interpretation of the PET. PET was co-registered to T1 MRI. A 10 % color gradation [blue (hypo), green, yellow, red (hyper)] with cerebellum set to yellow, was used to highlight areas of abnormality. The maximum standardized uptake value (SUV_{max}) was measured regionally in the mesial temporal, basal ganglia, and thalamic regions, and neo-cortex (rated over frontal, temporal, parietal, and occipital regions). The SUV_{max} was calculated as the voxel of highest SUV for a specified region. The SUV has been described as a ratio of radioactivity per a voxel expressed as a concentration (megaBecquerel per kilogram) divided by injected dose of radiation per kilogram of body mass [20]. Lack of arterial blood sampling prevented direct quantification of glucose metabolism. Because acute neurologic injury limited the utility of healthy subjects as a reference standard, we pre-specified that a 20 % relative difference in SUV_{max} ($rSUV_{max}$) compared with an internal control to ascertain differences in FDG uptake [21]. For focal abnormalities a contralateral homologous region was used to calculate the reference $rSUV_{max}$. Regions with altered metabolism were also compared to the total cerebellar SUV_{max}. If bilateral changes were ascertained on visual inspection, the contralateral reference was not available and we accordingly employed a threshold of 50 % increase of SUV_{max} relative to cerebellum, (a 99 % confidence interval assuming a normal distribution and with a 0.2 standard deviation) [22, 23]. Hypermetabolism and hypometabolism were classified as focal (present in a single region), regional (extending to subcortical or adjacent regions), or 3 diffuse (bilateral).

EEG Review

ACNS terminology-certified [1] clinical neurophysiologists blinded to clinical and PET data rated cEEG for discrete seizures, periodic discharges including modifiers frequency, location, amplitude, superimposed fast frequencies, rhythmic activity, sharp activity, and triphasic morphology. Discrepancies were resolved by consensus.

Determination of Status Epilepticus

No gold standard external to EEG exists to determine if a patient is in SE. We operationally differentiated electrographic SE from electroclinical SE using pre-specified published definitions. [24, 25]. We accordingly defined electrographic SE as meeting any of the

following criteria: (1a) a pattern of *>3-Hz* spike-wave, periodic discharges, or rhythmic activity or (1b) discrete electrographic seizures meeting Young criteria [25] without recovery of EEG background. We similarly defined electroclinical SE as meeting any of the following published criteria: (2a) an IIC pattern temporally associated with clonic activity; (2b) an IIC pattern associated with both clinical and EEG improvement following AED; or (2c) an IIC pattern following a single seizure in association with persistent encephalopathy [24, 25]. Clinical records were assessed by a neurologist blinded to cEEG and PET results for disease etiology and response to AED treatment.

Statistical Analysis

Categorical variables were analyzed for significance using Fisher-exact test. 95 % confidence intervals for proportions were generated using Wilson test with continuity correction [26]. Statistical analyses were performed using MATLAB 2013B (Natick, MA) and R 3.1.3 (The R Foundation for Statistical Computing; http://www.R-project.org.

Results

Patient Characteristics

Between 2005 and 2014, 18 inpatients met the selection criteria (mean age 56.6; range 14–83). All patients were on AEDs at the time of FDG-PET scanning Table 1 details patient, cEEG, and imaging characteristics, including determination of electrographic SE, electroclinical SE, or IIC patterns without SE. FDG-PET was hypermetabolic in 11 (61 %), hypometabolic in 5 (28 %) and normal in 2 (11 %) patients. Final diagnoses included structural lesions ($n = 8$; 44 %: of which 6 are ischemic or hemorrhagic strokes, 1 developmental venous anomaly, 1 mechanical injury), neuroinflammatory/neuroinfectious illness ($n = 7$; 39 %), decompensated epilepsy ($n = 2$), and Creutzfeldt–Jakob disease (CJD) ($n = 1$).

Relation of cEEG Patterns to PET Findings

Among IIC subjects, FDG-PET predicted SE (electrographic or electroclinical,) with 79 % sensitivity (95 % CI 53–93 %) and 100 % specificity (95 % CI 51–100 %); Fisher-exact $p = 0.01$. For the cohort of subjects without electrographic SE, FDG-PET predicted electroclinical SE with 80 % sensitivity (95 % CI 44–94 %) and 100 % specificity (95 % CI 51–100 %); Fisher-exact $p = 0.01$.

cEEG FDG-PET metabolism was assessed for its dependence on pre-specified candidate variables (Table 2). Certain cEEG features suggested high specificity for hypermetabolism (>1-Hz or high-amplitude PDs) or high sensitivity (PDs versus RDA) with insufficient statistical power to achieve significance.

FDG-PET was insensitive to electrographic or electroclinical SE in three patients. One patient had right parietal hypometabolism despite electroclinical SE diagnosed as epilepsia partialis continua (EPC) from a remote right parietal infarct with left facial twitching, 0.5-Hz right LPDs, and no evident electrographic seizures. A second patient diagnosed with CJD had diffuse hypometabolism with “electroclinical SE” diagnosed as a suspected clinical

seizure followed by persistent encephalopathy and 1-Hz GPDs. The third patient had NORSE of unknown etiology and diffuse hypometabolism despite electrographic SE diagnosed as discrete electrographic seizures with intervening 1-Hz GPDs.

Patterns of Metabolism

Three patterns of hypermetabolism were assessed: focal, regional, and diffuse. Figure 1 shows representative PETs of six subjects, two from each of hypermetabolism with the associated MR and EEG. Two subjects had diffuse hypermetabolism defined as regions of hypermetabolism in both hemispheres. Both presented with NORSE, one with LPDs and the other with 4-Hz GRDA. Five subjects had regional hypermetabolism, two with GPDs the others with LPDs. Subjects with regional hypermetabolism had pre-existing focal epilepsy (2), a structural lesion (2), or vasculitis (1). Four subjects had focal hypermetabolism all related to underlying structural lesion. Three had LPDs and the other had GPDs.

Five subjects had hypometabolism. In two patients, hypometabolism was diffuse (CJD, NORSE). The other three had regional or focal hypometabolism, two related to structural lesions and one with encephalitis.

Discussion

In this study, FDG-PET cerebral hypermetabolism similar to that described in cases of SE [5, 13, 18] was significantly more common among patients with IIC patterns fulfilling published criteria for electrographic SE or electroclinical SE than among patients with IIC patterns alone.

Although this cohort is the largest described with concomitant cEEG IIC patterns and concurrent FDG-PET, sample size ($n = 18$) limited conclusions about specific cEEG features. Additionally, FDG-PET was performed only in complicated cases with high clinical suspicion for SE this represents a referral bias. FDG-PET is not routinely performed in patients with critical neurologic illness for other reasons limiting the ability to generate a relevant set of control subjects. A prospective study of PET neuroimaging may more systematically identify IIC features (e.g., frequency, amplitude) most predictive of hypermetabolism. Additionally, it was difficult to gage the clinical response to AED therapy; clinical response was reviewed retrospectively and FDG-PET findings may have confounded the indication for further anti-seizure medications.

Potential limitations of FDG-PET imaging include spatial averaging from 5-mm resolution limits [20, 27] and temporal averaging during the 45-min uptake period. Examples in our cohort of these limitations may have included focal EPC dominated by surrounding hypometabolism (subject 16) and discrete seizures with intervening GPDs (subject 6). Technical advances with PET-MR and quantitative PET with arterial input function estimations have the potential to reduce the concerns with spatial and time averaging. A potential source of false positives is a hypermetabolic process independent of ictal activity such as encephalitis. Notably, we did not find FDG-PET hypermetabolism in any our cohort among seven subjects with neuroinflammatory/neuroinfectious disease; all were correctly classified except one false negative.

Conclusion

SE and the IIC represent a spectrum of neurophysiologic dysfunction. Some IIC patterns are associated with AED-responsive reversible cerebral dysfunction due to deep-seated or undetected ictal zones or “burned out” SE with persistently altered metabolism. Here, we demonstrate that the metabolic effect of IIC in patients with suspected SE without definite electrographic features is similar to the metabolic features of electrographic SE and is not routinely explained by neuroinflammatory or neuroinfectious disease alone. Figure 2 is our adaptation of a diagram describing the IIC initially put forth by Chong and Hirsch [24]. This diagram helps conceptualize the role of metabolism in evaluating SE and the IIC. This study reinforces prior work which raises the possibility of ancillary biomarkers for SE and develops the concept of “electro-metabolic” status epilepticus. We put forth FDG-PET as another candidate radiologic biomarker of status epilepticus.

References

1. Hirsch LJ, LaRoche SM, Gaspard N, et al. American Clinical Neurophysiology Society’s standardized critical care EEG terminology: 2012 version. J Clin Neurophysiol. 2013; 30:1–27. [PubMed: 23377439]
2. Orta DS, Chiappa KH, Quiroz AZ, Costello DJ, Cole AJ. Prognostic implications of periodic epileptiform discharges. Arch Neurol. 2009; 66:985–91. [PubMed: 19667220]
3. Walsh JM, Brenner RP. Periodic lateralized epileptiform discharges–long-term outcome in adults. Epilepsia. 1987; 28:533–6. [PubMed: 3653057]
4. Claassen J, Jette N, Chum F, et al. Electrographic seizures and periodic discharges after intracerebral hemorrhage. Neurology. 2007; 69:1356–65. [PubMed: 17893296]
5. Claassen J. How I treat patients with EEG patterns on the ictal-interictal continuum in the neuro ICU. Neurocrit Care. 2009; 11:437–44. [PubMed: 19851892]
6. Coeytaux A, Jallon P, Galobardes B, Morabia A. Incidence of status epilepticus in French-speaking Switzerland: (EPISTAR). Neurology. 2000; 55:693–7. [PubMed: 10980736]
7. Knake S, Rosenow F, Vescovi M, et al. Incidence of status epilepticus in adults in Germany: a prospective, population-based study. Epilepsia. 2001; 42:714–8. [PubMed: 11422324]
8. Treiman DM, Walton NY, Kendrick C. A progressive sequence of electroencephalographic changes during generalized convulsive status epilepticus. Epilepsy Res. 1990; 5:49–60. [PubMed: 2303022]
9. Claassen J, Perotte A, Albers D, et al. Nonconvulsive seizures after subarachnoid hemorrhage: multimodal detection and outcomes. Ann Neurol. 2013; 74:53–64. [PubMed: 23813945]
10. Hajek M, Antonini A, Leenders KL, Wieser HG. Epilepsia partialis continua studied by PET. Epilepsy Res. 1991; 9:44–8. [PubMed: 1909238]
11. Engel J Jr, Kuhl DE, Phelps ME. Patterns of human local cerebral glucose metabolism during epileptic seizures. Science. 1982; 218:64–6. [PubMed: 6981843]
12. Meltzer CC, Adelson PD, Brenner RP, et al. Planned ictal FDG PET imaging for localization of extratemporal epileptic foci. Epilepsia. 2000; 41:193–200. [PubMed: 10691116]
13. Stayman A, Abou-Khalil B. FDG-PET in the diagnosis of complex partial status epilepticus originating from the frontal lobe. Epilepsy Behav. 2011; 20:721–4. [PubMed: 21440509]
14. Siclari F, Prior JO, Rossetti AO. Ictal cerebral positron emission tomography (PET) in focal status epilepticus. Epilepsy Res. 2013; 105:356–61. [PubMed: 23582605]
15. Chugani HT, Shewmon DA, Khanna S, Phelps ME. Interictal and postictal focal hypermetabolism on positron emission tomography. Pediatr Neurol. 1993; 9:10–5. [PubMed: 8452593]
16. Raichle ME, Gusnard DA. Appraising the brain’s energy budget. Proc Natl Acad Sci USA. 2002; 99:10237–9. [PubMed: 12149485]

17. Franck G, Sadzot B, Salmon E, et al. Study of cerebral metabolism and blood flow in partial complex epilepsy and status epilepticus in man using positron emission tomography. Rev Electroencephalogr Neurophysiol Clin. 1986; 16:199–216. [PubMed: 3492737]
18. Handforth A, Cheng JT, Mandelkern MA, Treiman DM. Markedly increased mesiotemporal lobe metabolism in a case with PLEDs: further evidence that PLEDs are a manifestation of partial status epilepticus. Epilepsia. 1994; 35:876–81. [PubMed: 8082637]
19. Kim HY, Kim JY, Kim GU, Han HJ, Shin DI. Alien hand syndrome after epilepsia partialis continua: FDG PET and MRI studies. Epilepsy Behav. 2012; 23:71–3. [PubMed: 22100067]
20. Granov, AM., Titutin, LA., Schwarz, T. Positron emission tomography. Berlin: Springer; 2008.
21. Kinahan PE, Fletcher JW. Positron emission tomography-computed tomography standardized uptake values in clinical practice and assessing response to therapy. Semin Ultrasound CT MR. 2010; 31:496–505. [PubMed: 21147377]
22. Hikima A, Mochizuki H, Oriuchi N, Endo K, Morikawa A. Semiquantitative analysis of interictal glucose metabolism between generalized epilepsy and localization related epilepsy. Ann Nucl Med. 2004; 18:579–84. [PubMed: 15586631]
23. Ng S, Villemagne VL, Berlangieri S, et al. Visual assessment versus quantitative assessment of 11C-PIB PET and 18F-FDG PET for detection of Alzheimer's disease. J Nucl Med. 2007; 48:547–52. [PubMed: 17401090]
24. Chong DJ, Hirsch LJ. Which EEG patterns warrant treatment in the critically ill? Reviewing the evidence for treatment of periodic epileptiform discharges and related patterns. J Clin Neurophysiol. 2005; 22:79–91. [PubMed: 15805807]
25. Young GB, Jordan KG, Doig GS. An assessment of nonconvulsive seizures in the intensive care unit using continuous EEG monitoring: an investigation of variables associated with mortality. Neurology. 1996; 47:83–9. [PubMed: 8710130]
26. Newcombe RG. Two-sided confidence intervals for the single proportion: comparison of seven methods. Stat Med. 1998; 17:857–72. [PubMed: 9595616]
27. Moses WW. Fundamental limits of spatial resolution in PET. Nucl Instrum Methods Phys Res A. 2011; 648(Supplement 1):S236–40. [PubMed: 21804677]

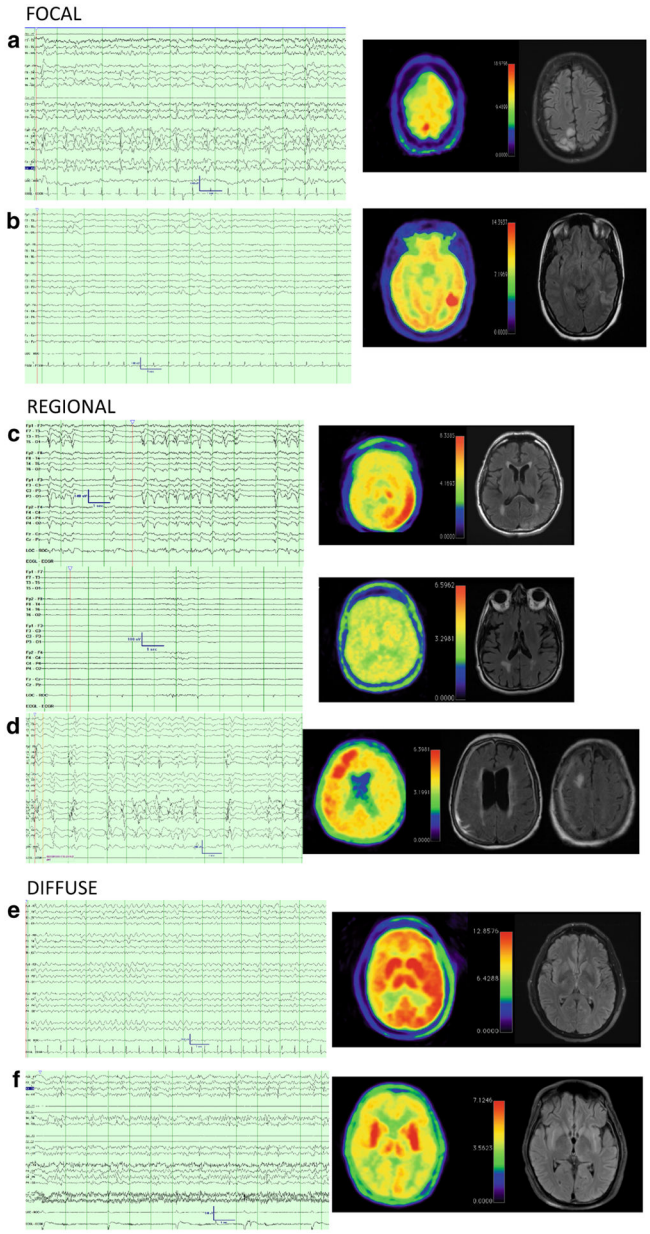

Fig. 1.

Representative cases of patterns of PET hypermetabolism with corresponding electrographic and MR data. 13-s cEEG samples and FDG-PET imaging [rainbow color scheme; 10 % gradations from hypometabolic (*blue*) through *green* and *yellow* to hypermetabolic (*red*), cerebellum set to yellow, L demarcates left orientation] and FLAIR MR images for six subjects. **a**, **b** are representative cases of focal hypermetabolism. **a** (SUBJ 3) is a 32-year-old woman with a history of peri-natal stroke that presented with epilepsia partialis continua, MRI had T2 hyperintensity near the remote infarct with corresponding PET hypermetabolism in the same region. EEG had LPDs and intermittent discrete seizures. She required surgery to remove the ictal focus, which resulted in cessation of seizure activity, but a worsened hemiparesis. **b** (SUBJ 1) Is a 25-year-old woman that presented with convulsive

status epilepticus transitioning to persistent encephalopathy with initial AED treatment. cEEG had persistent 0.5 Hz right posterior quadrant LPDs, MRI revealed a posterior temporal T2 hyperintensity with an adjacent developmental venous anomaly. PET revealed focal hypermetabolism in the region of the MRI abnormality. Treatment was escalated with IV sedation and patient made a full recovery. Follow-up MRI revealed a resolution of T2 hyperintensity. **c**, **d** are representative cases of regional hypermetabolism. **c** (SUBJ 15) is a 77-year-old man presenting with hypertension and T2 hyperintensities of the left occipital/parietal cortex and scattered white matter T2 hyperintensities, DWI changes, and microhemorrhages. Initial cEEG revealed discrete electrographic seizures. After anti-seizure medication (*top panel*), cEEG displayed an IIC pattern (*left* LPDs) associated with focal FDG-PET hypermetabolism in left parietal, occipital, posterior-frontal right thalamic regions. (*Bottom panel*) Anesthetic burst-suppression was employed and repeat PET yielded resolution of hypermetabolism 12 days later concurrent with burst-suppression on cEEG. LPDs subsequently resumed with weaning sedation and his persistent encephalopathy prompted family to elect palliative care, autopsy revealed inflammatory cerebral amyloid angiopathy. **d** (SUBJ 13) is an 84-year-old woman with dementia s/p VP shunt placement for NPH that developed discrete focal seizures, which resolved with AED treatment. Patient had persistent encephalopathy and was found to have LPDs on cEEG and regional hypermetabolism on PET. MRI revealed pachymeningeal thickening and enhancement as well as a right frontal focal area of hemorrhage and surrounding T2 hypermetabolism along the shunt tract. Patient did not improve and was transitioned to palliative care. **e**, **f** are representative cases of diffuse hypermetabolism. **e** (SUBJ 11) is 44-year-old man with subacute cognitive decline presenting with clinical seizures and worsening encephalopathy. cEEG had 4 Hz GRDA and diffuse (L > R) cortical and subcortical hypermetabolism. Found to have VGKC antibody, return to baseline with AEDs and IVIG. **f** (SUJB 5) is a 23-year-old man presenting with NORSE, his clinical seizures improved with treatment, but clinical deficits persisted. cEEG revealed LPDs. PET has bilateral hypermetabolism primarily in the basal nuclei. MRI was normal other than mild generalized volume loss. Patient recovered with a residual modest spastic tetraparesis and cognitive recovery. Etiology of illness remains cryptogenic (Color figure online)

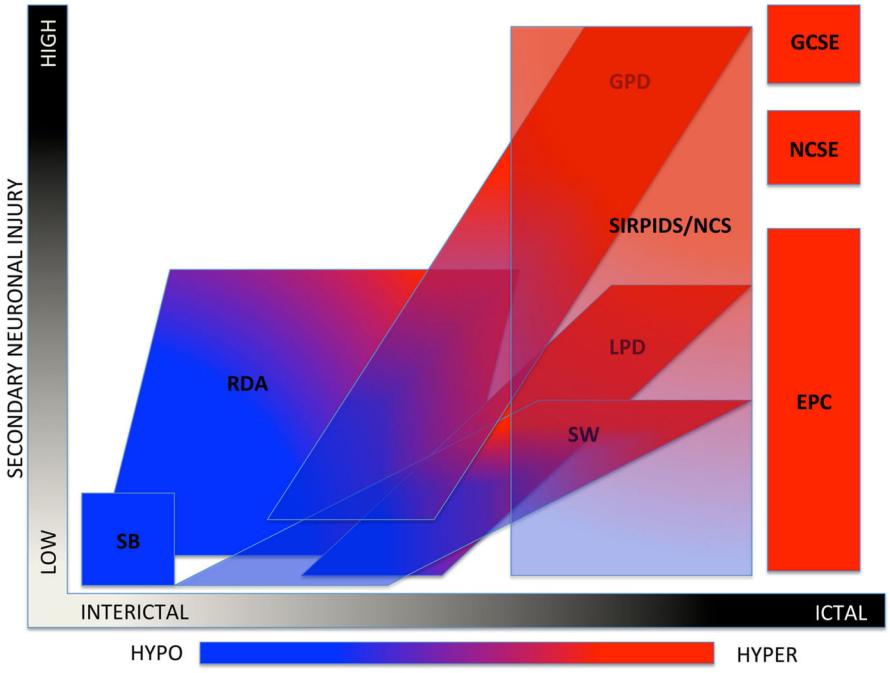

Fig. 2.

The ictal-interictal-injury-metabolism continuum. This diagram is a graphic conceptualization adapted from Chong and Hirsh [24] using the current ACNS terminology and with the addition of PET metabolism ranging from hypo/normo metabolic in *blue* to hypermetabolic in *red*. This conceptualization is meant only to reflect scalp EEG patterns. *X*-axis represents the spectrum of interictal to ictal, i.e., the spectrum of cerebral dysfunction, which is potentially reversible with anti-seizure treatment. *Y*-axis is secondary neuronal damage attributable to the EEG pattern. *SB* suppression burst, *RDA* rhythmic delta activity, *LPD* lateralized periodic discharges, *SW* spike wave, *GPD* generalized periodic discharges, *SIRPIDs* stimulus-induced rhythmic, periodic, or ictal discharges, *NCS* non-convulsive seizures, *GCSE* generalized convulsive status epilepticus, *NCSE* non-convulsive electrographic status epilepticus, *EPC* epilepsia partialis continua, *HYPO* hypometabolism, *HYPER* hypermetabolism (Color figure online)

Neurocrit Care. Author manuscript; available in PMC 2017 June 20.

Table 1

Patient Characteristic

Subject	SE	PET	Etiology	Pattern	Freq(Hz)	Amplitude	Duration	AEDs	Time
1	2b	F-Hyper	Vascular malformation	GPD	0.5	High	Long	LEV, PHT, LCM	7
2	2b	F-Hyper	Infarct	LPD	1	Medium	Long	LEV, PHT, LCM, CZN	4
3	1b	F-Hyper	Infarct	LPD	1.5	Medium	Long	LEV, LMT, TPM, LZM, PHT, CZN	1
4	2b	R-Hyper	Focal epilepsy	LPD	0.5	Medium	Long	LEV, PHT, LCM, MG	3
5	2b	D-Hyper	NORSE	LPD	2	Low	Long	PHB, LCM, LEV, CZN, TPM	99
6	1b	D-Hypo	NORSE	GPD	1	Medium	Intermediate	FBM, TPM, LEV, PHT	11
7	0	N	Limbic encephalitis	GRDA	3	Medium	Brief	LEV, LCM, TPM, PHB, CZN	26
8	2c	D-Hypo	CJD	GPD	1	Medium	Long	LEV, PHT	5
9	1b	F-Hyper	Lobar hemorrhage	LPD	1	High	Intermediate	LEV, LCM, PHT	30
10	2b	R-Hyper	Generalized epilepsy	GPD	2.5	High	Intermediate	CBZ, VPA, LMT, LEV, LCM, MZM	2
11	1a	D-Hyper	VGKC encephalitis	GRDA	4	Medium	Intermediate	LEV, PHT	4
12	0	N	NORSE	GRDA	1.5	Medium	Long	PHT, LEV, LCM	11
13	2c	R-Hyper	Intracranial hemorrhage	GPD	1	Medium	Long	LEV, PHT, LZM	5
14	2b	R-Hyper	Infarct	LPD	1	Medium	Long	PHT, LCM, LEV, TPM	7
15	2c	R-Hyper	PRES/CAA vasculitis	LPD	2.5	Medium	Intermediate	LEV, VPA, OXC, CZN	9
16	2a	F-Hypo	Lobar hemorrhage	LPD	0.5	Medium	Intermediate	TPM, PHB, LEV	4
17	0	F-Hypo	WNV encephalitis	GRDA	2	Medium	Very brief	LCM, PHT	10
18	0	R-Hypo	Infarct	LPD	0.5	Low	Intermediate	LEV, VPA	12

0 no SE, *1a* electrographic SE at the time of PET acquisition due to SW, *PD* or RDA exceeding 3-Hz frequency, *1b* electrographic SE at the time of PET acquisition due to multiple discrete electrographic seizures without recovery of EEG background, *2a* electroclinical SE at the time of PET acquisition due to an EEG IIC pattern temporally associated with clonic activity, *2b* electroclinical SE at the time of PET acquisition due to an EEG IIC pattern that demonstrated temporal clinical and EEG improvement following medication administration, *2c* electroclinical SE at the time of PET acquisition due to an EEG IIC pattern associated with persistent encephalopathy following a clinical seizure, *CJD* Creutzfeldt–Jakob disease, *D-Hypo* diffuse hypometabolism, *D-Hyper* diffuse hypermetabolism, *F-Hypo* focal hypometabolism, *F-Hyper* focal hypermetabolism, *Freq* Frequency, *N* normal, *NORSE* new-onset refractory status epilepticus, *R-Hypo* regional hypometabolism, *R-Hyper* regional hypermetabolism, *SE* status epilepticus, *Subject* subject number, *AEDs* during uptake period of PET, note IV infusion were held, *LEV* levetiracetam, *PHT* phenytoin, *LCM* lacosamide, *CZN* clonazepam, *MG* magnesium, *TPM* topiramate, *FBM* felbamate, *CBZ* carbamazepine, *VPA* valproic acid, *MZM* midazolam, *LZM* lorazepam, *OXC* oxcarbazepine, *PHB* phenobarbital, *Time* time from admission to PET scan measured in days

Table 2

Predictors of PET Hypermetabolism

cEEG risk factor	Sensitivity (95 % CI)	Specificity (95 % CI)	Accuracy (95 % CI)	*p* value
Periodic discharges				
PD[a]	0.91 (0.57–0.99)	0.43 (0.12–0.80)	0.72 (0.46–0.89)	0.25
LPD[b]	0.70 (0.35–0.92)	0.50 (0.10–0.91)	0.64 (0.35–0.86)	0.58
Duration, long[c]	0.70 (0.35–0.92)	0.75 (0.22–0.99)	0.71 (0.41–0.90)	0.25
Amplitude, high[c]	0.30 (0.08–0.65)	1.00 (0.40–1.00)	0.57 (0.30–0.81)	0.36
Superimposed fast activity[c]	0.40 (0.14–0.73)	0.50 (0.10–0.91)	0.43 (0.19–0.70)	1.00
Frequency				
>1 Hz	0.40 (0.14–0.73)	1.00 (0.40–1.00)	0.57 (0.30–0.81)	0.25
>2.5 Hz	0.18 (0.03–0.52)	1.00 (0.56–1.00)	0.56 (0.32–0.78)	0.49
Seizures	0.27 (0.07–0.60)	0.86 (0.42–0.99)	0.50 (0.27–0.73)	1.00
Status epilepticus				
Electrographic SE or electroclinical SE (vs. IIC with no SE)	0.79 (0.53–0.93)	1.00 (0.51–1.00)	0.83 (0.61–0.94)	**0.01**
Electroclinical SE without electrographic SE (vs. IIC with no SE)	0.80 (0.44–0.94)	1.00 (0.51–1.00)	0.86 (0.60–0.96)	**0.01**

Significant *p*-values (<0.05) are in bold

PD periodic discharges, *GPD* generalized periodic discharges, *LPD* lateralized periodic discharges, *RDA* rhythmic delta activity

[a]Versus RDA

[b]Versus GPD

[c]Evaluated only for subjects with PDs